DOI: 10.1002/ejic.200600334

Syntheses, Structures and Near-IR Luminescent Studies on Ternary Lanthanide (Er^{III}, Ho^{III}, Yb^{III}, Nd^{III}) Complexes Containing 4,4,5,5,6,6,6-Heptafluoro-1-(2-thienyl)hexane-1,3-dionate

Li-Ning Sun,[a,b,c] Jiang-Bo Yu,[a] Guo-Li Zheng,[a,c] Hong-Jie Zhang,*[a] Qing-Guo Meng,[a] Chun-Yun Peng,[a] Lian-She Fu,[a] Feng-Yi Liu,[a] and Ying-Ning Yu[a]

Keywords: Lanthanides / Luminescence / Optical amplification

The ligand Hhfth [4,4,5,5,6,6,6-heptafluoro-1-(2-thienyl)hexane-1,3-dione], which contains a heptafluoropropyl group, has been used to synthesize several new ternary lanthanide complexes (Ln = Er, Ho, Yb, Nd) in which the synergistic ligand is 1,10-phenanthroline (phen) or 2,2′-bipyridine (bipy). The two series of complexes are [Ln(hfth)$_3$phen] [abbreviated as (Ln)**1**, where Ln = Er, Ho, Yb] and [Ln(hfth)$_3$bipy] [abbreviated as (Ln)**2**, where Ln = Er, Ho, Yb, Nd]. Members of the two series have been structurally characterized. The growth morphology, diffuse reflectance (DR) spectra, thermogravimetric analyses, and photophysical studies of these complexes are described in detail. After ligand-mediated excitation of the complexes, they all show the characteristic near-infrared (NIR) luminescence of the corresponding Ln^{3+} ions (Ln = Er, Ho, Yb, Nd). This is attributed to efficient energy transfer from the ligands to the central Ln^{3+} ions, i.e. an antenna effect. The heptafluorinated substituent in the main hfth sensitizer serves to reduce the degree of vibrational quenching. With these NIR-luminescent lanthanide complexes, the luminescent spectral region from 1300 to 1600 nm, which is of particular interest for telecommunication applications, can be covered completely.
(© Wiley-VCH Verlag GmbH & Co. KGaA, 69451 Weinheim, Germany, 2006)

Introduction

There has been increasing interest in the use of near-infrared (NIR) light, which is one of the best strategies to obtain high-resolution pictures of deep tissues as NIR light diffracts much less than visible light [diffraction is proportional to $1/(\lambda)^{SP}$, SP = scattering power].[1] Recently, the lanthanide ions that are emissive in the NIR region of the spectrum (800–1700 nm), such as Yb^{III}, Nd^{III}, Ho^{III}, and Er^{III}, have received much attention. Interest in the photophysical properties of these lanthanide ions mainly stems from the following three points. First, the Yb^{3+} ion emission occurs in the NIR region (approximately 1000 nm) where biological tissues and fluids (e.g. blood) are relatively transparent, thus the development of Yb^{3+} ion luminescence for various analytical and chemosensor applications is promising. Second, Nd-containing systems have been regarded as the most popular infrared luminescent materials for application in laser systems (the basis of the common 1064-nm laser). Third, two telecommunication windows for amplification are commonly used for long-distance communication, one at 1.3 μm using Nd emission and the other at 1.5 μm using Er or Ho emission.[2]

However, the low optical cross-section due to the forbidden nature of the 4f→4f transitions of these NIR-luminescence lanthanide ions results in inefficient direct excitation.[3] Since the discovery that energy transfer from the triplet state of an organic ligand can efficiently sensitize the emissive states of lanthanide ions,[4] there has been considerable effort devoted to designing ligands that optimize this energy transfer and thus give efficient lanthanide luminescence. β-Diketones are most commonly used for the complexation of lanthanide ions. Because of their potential applications, tris- and tetrakis(β-diketonato)lanthanides(III) are the most widely studied complexes of the 4f-element series.[5] In addition, noncharged ligands like 1,10-phenanthroline (phen) or 2,2′-bipyridine (bipy) can serve as the synergistic agent, since an important issue in the design of NIR-emitting lanthanide complexes is to prevent water molecules from binding to the lanthanide ions. Sensitizer-functionalized Eu^{3+} and Tb^{3+} complexes have already been applied as long-lasting luminescent probes in time-resolved fluoroimmunoassays,[6] whereas sensitizer-functionalized complexes of the NIR-emitting lanthanide ions Er^{3+}, Yb^{3+}, Nd^{3+}, and especially Ho^{3+}, are less well studied. These com-

[a] Key Laboratory of Rare Earth Chemistry and Physics, Changchun Institute of Applied Chemistry, Chinese Academy of Sciences,
Changchun, 130022, P. R. China
Fax: +86-431-5262127
E-mail: hongjie@ns.ciac.jl.cn
[b] State Key Laboratory of Structural Chemistry, Fujian Institute of Research on the Structure of Matter, Chinese Academy of Sciences,
Fuzhou, 350002, P. R. China
[c] Graduate School of the Chinese Academy of Sciences,
Beijing, P. R. China
Supporting information for this article is available on the WWW under http://www.eurjic.org or from the author.

 © 2006 Wiley-VCH Verlag GmbH & Co. KGaA, Weinheim

plexes are very promising not only for application in fluoroimmunoassays, but also for use in laser systems and for amplification of light.[2]

It is well established that the NIR-emitting Ln^{3+} ions are particularly prone to vibrational deactivation. Species containing high-energy oscillators, such as C–H and O–H bonds (typically found in the ligand), are able to quench the metal excited states nonradiatively, thereby leading to lower luminescence intensities and shorter excited-state lifetimes. The replacement of C–H bonds with C–F bonds is important in the syntheses of lanthanide complexes with efficient photoemission properties.[5,7] According to the literature reported previously, the replacement of C–H bonds in a β-diketone ligand with lower-energy C–F oscillators is able to lower the vibration energy of the ligand, which decreases the energy loss caused by ligand vibration and enhances the emission intensity of the lanthanide ion.[8] Due to the heavy-atom effect,[7e] which facilitates intersystem crossing, the lanthanide-centered luminescent properties are enhanced.[9] It has been reported that the fluorescence quantum yield of a europium(III) complex increases with more fluorinated alkyl groups on the β-diketonate ligand.[5,8c] More fluorinated β-diketones form more stable ternary complexes with Lewis bases in organic solvents.[7f] In this work, the β-diketone ligand Hhfth [4,4,5,5,6,6,6-heptafluoro-1-(2-thienyl)hexane-1,3-dione], which contains a long perfluoroalkyl chain, is used as the main sensitizer for synthesizing new NIR-emitting lanthanide complexes.

In this context, and in connection with our interest in photoluminescence and electroluminescence,[2a,8a,9,10] we are interested in studying the crystal structures and luminescence properties of lanthanide complexes. Herein, we report the syntheses and structures of new sensitizer-functionalized NIR-luminescence complexes [$Ln(hfth)_3phen$] [abbreviated as (Ln)**1**, where Ln = Er, Ho, Yb] and [$Ln(hfth)_3bipy$] [abbreviated as (Ln)**2**, where Ln = Er, Ho, Yb, Nd], which contain the hfth ligand with a heptafluoropropyl group (see Figure S1, Supporting Information). The properties of these complexes were investigated using diffuse reflectance (DR) spectra and thermogravimetric analyses, and the photophysical properties were studied in detail and compared with those of the [$Ln(hfth)_3(H_2O)_2$] complexes.

Results and Discussion

Design and Preparation of Complexes (Ln)1 and (Ln)2

The molar ratio of the lanthanide ion and the β-diketonate investigated was determined to be 1:3 or 1:4. Three possible types of lanthanide complexes can be designed depending on the ratio:[11,12] (1) When the ratio is 1:3, a simple tris(complex) can be obtained with three hfth ligands coordinated to one lanthanide ion. However, the six oxygen atoms from three hfth ligands are not sufficient to complete the coordination number requirement of a lanthanide ion (typically 8 or 9). Thus, the tris(complex) usually contains water or other solvent molecules in the first coordination sphere, which is disadvantageous for obtaining high luminescence intensity. (2) When a metal/ligand ratio of 1:4 is used, the tetrakis(complex) can be obtained. Although the tetrakis(complexes) usually show much higher luminescence intensity, the disadvantage is that a single positively charged counterion is needed to assure the electrical neutrality of the complex. This is problematic in the design of electroluminescent devices for charged species. The above two types leave us with the third option. (3) In addition to a metal/ligand ratio of 1:3, a Lewis base such as phen or bipy is added to give a Lewis base adduct of the tris(complex). The function of phen or bipy is to saturate the coordination sphere of the lanthanide ion and also to absorb excitation energy that can be transferred to the excited states of the lanthanide ion.

It is well known that the positions of the luminescence bands in the spectrum are characteristic for a specific lanthanide ion. This means that the given organic ligands that are capable of coordinating with different lanthanide ions can serve various applications operating at different wavelengths simply by changing the central lanthanide ion (in our case Ln = Er, Ho, Yb, Nd).

Crystal Structures

The structure of the lanthanide complex is essential to understand the energy transfer from the coordinated ligands to the central lanthanide ion. Therefore, a considerable number of these complexes with various β-diketonates have been structurally characterized by X-ray crystallography since the 1970s. In the present work, the single-crystal X-ray diffraction studies revealed isostructural crystals (orthorhombic, $Z = 8$) for complexes (Ln)**1** and (Ln)**2** whose crystals fall in the same *Pbca* space group. Thus, only the structures of (Er)**1** and (Yb)**2** will be described in detail as examples.

The crystal structure of (Er)**1**, with the numbering scheme, is displayed in Figure 1a. Analysis of the crystal structure indicates that the central Er^{3+} ion is eight-coordinate, with six oxygen atoms from three hfth ligands and two nitrogen atoms from the phen ligand. From the coordination angles, the coordination geometry may be described as a square antiprism, one of the two most stable eight-coordinate polyhedra (shown in Figure 1b). The crystal structure of (Yb)**2** (Figure 2a) is similar. The coordination number of the central Yb^{3+} ion is also eight, with six oxygen atoms from three hfth ligands and two nitrogen atoms from the bipy ligand. The coordination polyhedron can also be regarded as a square antiprism (see Figure 2b). For these two complexes, the Ln–O bonds adjacent to the thienyl ring are slightly longer than the others, which is probably due to the inductive effect of the fluorine atoms on the alkyl chain. In the β-diketone rings of the lanthanide complexes, all of the average distances for the C–C and C–O bonds are shorter than a single bond but longer than a double bond. This can be explained by the fact that there is conjugation between the thienyl ring and the coordinated β-diketonate, which

 © 2006 Wiley-VCH Verlag GmbH & Co. KGaA, Weinheim

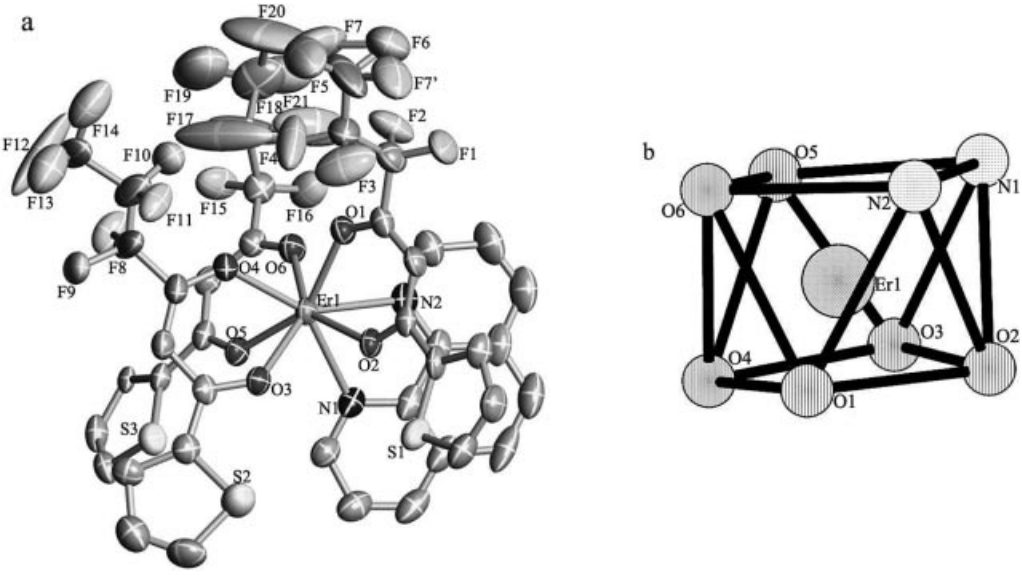

Figure 1. (a) ORTEP plot for (Er)**1** with ellipsoids drawn at the 30% probability level. Hydrogen atoms have been omitted for clarity. (b) Coordination polyhedron of the Er^{III} ion.

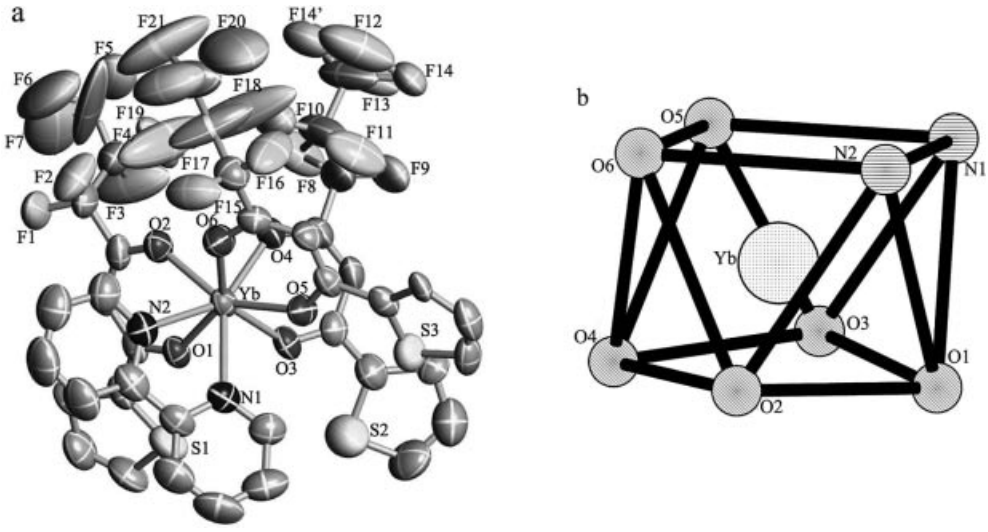

Figure 2. ORTEP plot for (Yb)**2** with ellipsoids drawn at the 30% probability level. Hydrogen atoms have been omitted for clarity.

leads to the delocalization of electron density of the coordinated β-diketonate chelate ring. However, the C–C bond lengths near the fluorine atoms are close to that of a C=C bond, which is due to the inductive effect of the fluorine atoms.[13] The central Ln^{3+} ion is completely surrounded by the bulky anionic ligand hfth and the synergistic ligands phen [for (Ln)**1**] or bipy [for (Ln)**2**], and this encapsulated structure therefore meets the structural requirements of a lanthanide luminescent sensor[14] by protecting the metal ion from vibrational coupling and increasing the light absorption cross-section by the "antenna effect".

The average Ln–O and Ln–N bond lengths in the crystals are shown in Table 1, where it can be seen that the average Ln–O and Ln–N bond lengths decrease from Ho to Yb [for (Ln)**1**] and from Nd to Yb [for (Ln)**2**] due to the so-called "lanthanide contraction". It can also be seen that the cell volume contracts by about 3.81% for (Ln)**1** when the lanthanide ion changes from Ho to Yb and about 1.58% for (Ln)**2** when the lanthanide ion changes from Nd to Yb.

Table 1. Average Ln–O and Ln–N bond lengths [Å] for (Ln)**1** and (Ln)**2**.

	(Ho)**1**	(Er)**1**	(Yb)**1**	(Nd)**2**	(Ho)**2**	(Yb)**2**
Ln–O	2.310	2.296	2.276	2.393	2.311	2.279
Ln–N	2.551	2.520	2.501	2.633	2.532	2.492

Observed Growth Morphology

Of the single crystals obtained, all the (Ln)**1** crystals show a regular, diamond-like shape whereas the shape of the (Ln)**2** crystals is irregular. We are not sure about the

 © 2006 Wiley-VCH Verlag GmbH & Co. KGaA, Weinheim

reason for this phenomenon, although we think that it may be due to the different molecular structures of phen and bipy. All atoms of the phen molecule are in the same conjugate area, yet those of the bipy molecule are not. Microscope pictures of a single crystal of (Er)**1** with a diamond shape are shown in Figure 3 to illustrate the growth morphology that is representative for crystals of (Ln)**1** but not for those of (Ln)**2**. A schematic sketch of each crystal selected is shown in Figure 3 (right), which reveals the growth habit of the crystals.

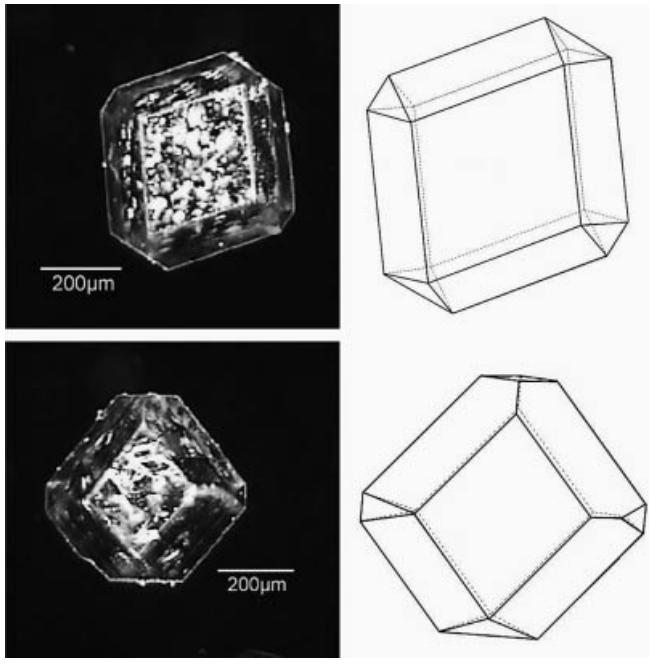

Figure 3. Microscope images and corresponding sketches of the (Er)**1** crystals grown from the ethanol/acetone mother liquor.

DR Spectra

The DR Spectra of (Ln)**1** and (Ln)**2** (Ln = Er, Ho, Yb, Nd) are shown in Figure 4. In the UV region of the DR curves (200–400 nm), all broad absorption bands are observed and can be assigned to electronic transitions from the ground-state level S_0 to the excited level S_1 of the organic ligands. In the region above 400 nm in these figures, each absorption band corresponds to a characteristic transition between two spin-orbit coupling levels of the lanthanide ion (see the insets of Figure 4). Based on the energy level scheme of each ion, these bands can be assigned to the transitions from the ground levels $^4I_{15/2}$, $^5I_8$, $^2F_{7/2}$, and $^4I_{9/2}$ to the higher energy levels for the erbium, holmium, ytterbium, and neodymium complexes, respectively.[15–17]

Photophysical Properties

In 1942, Weissman reported that lanthanide luminescence can be improved by using an intramolecular energy transfer, the so-called "antenna effect".[4a] Because the intraconfigurational f↔f transitions are forbidden, absorption of the lanthanide(III) is very weak. In most cases, one can use the excitation of strongly absorbing ligands followed by energy transfer to promote the lanthanide ion to the emitting state.[18] Each of the lanthanide ions used in the course of this work is known to exhibit one or more spectral emission bands in the 800–1700 nm region. Thus, to provide a clear understanding of the photophysics and luminescence properties of these new series of lanthanide complexes, the excitation and emission spectra of each complex as well as the absorption spectra of the ligands were characterized and discussed in detail.

The excitation spectra of (Ln)**1** and (Ln)**2** (Ln = Er, Ho, Yb, Nd) and the absorption spectra of the ligands (phen,[2a] Hhfth, and bipy) were obtained (Figure S2, Supporting Information). As is clearly visible in this figure, there are overlaps between the excitation band of each lanthanide complex and the absorption bands of Hhfth and phen (or Hhfth and bipy), which indicates the typical sensitization of the Ln^{3+} ions by the two organic ligands[19] and thus confirms that the Ln^{3+} ions are surrounded by hfth and phen (or hfth and bipy) in the complexes.[3a,20] It is also worth noting that the overlap between the absorption band of Hhfth and the lanthanide excitation band is larger than that between the absorption band of phen (or bipy) and the excitation band, which suggests that the antenna effect of the hfth ligand is more efficient than that of the synergistic ligand (phen or bipy). Thus, it is reasonable to deduce that the intramolecular energy transfer in the lanthanide complexes mainly occurs between the hfth ligand and the Ln^{3+} ions.[13]

The emission studies were carried out in the NIR region on all of these complexes upon excitation of the ligand absorption bands, followed by NIR emission for the Er^{3+}, Ho^{3+}, Yb^{3+}, and Nd^{3+} complexes where the synergistic ligand is phen or bipy. Using identical experimental settings (slit width, integration time, excitation wavelength, sampling interval), the direct comparison of the emission intensity of the NIR luminescence for the same lanthanide ion with different synergistic ligands was investigated.

Erbium

As is shown in Figure S2, the excitation spectra of the (Er)**1** and (Er)**2** complexes were obtained by monitoring the characteristic emission of the Er^{3+} ion at 1541 nm. In the excitation spectra, a broad band ranging from 260 to 435 nm for (Er)**1** and a broad band from 235 to 430 nm for the (Er)**2** complex are observed. The two broad bands can be assigned to the absorption of the organic ligands, which is in agreement with the DR spectra mentioned above (Figure 4a). Some small bands, originating from f–f absorption transitions of the Er^{3+} ion, are also observed in the excitation spectra of the two complexes. They correspond to the energy transitions $^4I_{15/2}\rightarrow{}^4F_{7/2}$ [492 nm for (Er)**1** and 486 nm for (Er)**2**] and $^4I_{15/2}\rightarrow{}^2H_{11/2}$ [528 nm for (Er)**1** and 524 nm for (Er)**2**], which is also in agreement with the DR spectra (Figure 4a).

Excitation of the ligand absorption bands at 397 nm resulted in the emission spectra (Figure 5) of the two Er complexes. For (Er)**1** and (Er)**2**, the emission bands cover large

 © 2006 Wiley-VCH Verlag GmbH & Co. KGaA, Weinheim

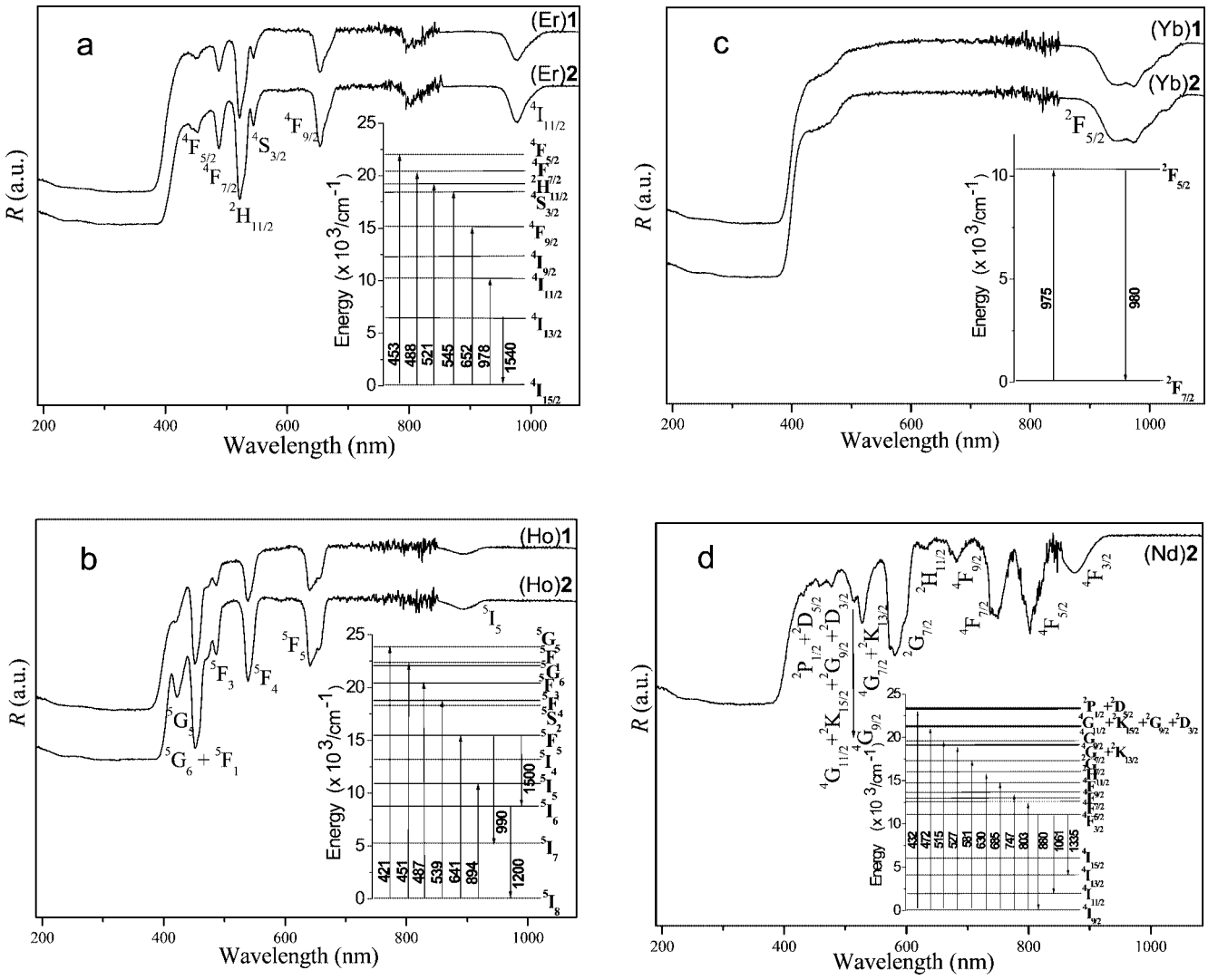

Figure 4. DR spectra of (Er)**1** and (Er)**2** (a), (Ho)**1** and (Ho)**2** (b), (Yb)**1** and (Yb)**2** (c), and (Nd)**2** (d). The insets show the energy level diagrams of Er^{3+}, Ho^{3+}, Yb^{3+}, and Nd^{3+}. The transitions of the bands [nm] are indicated by arrows.

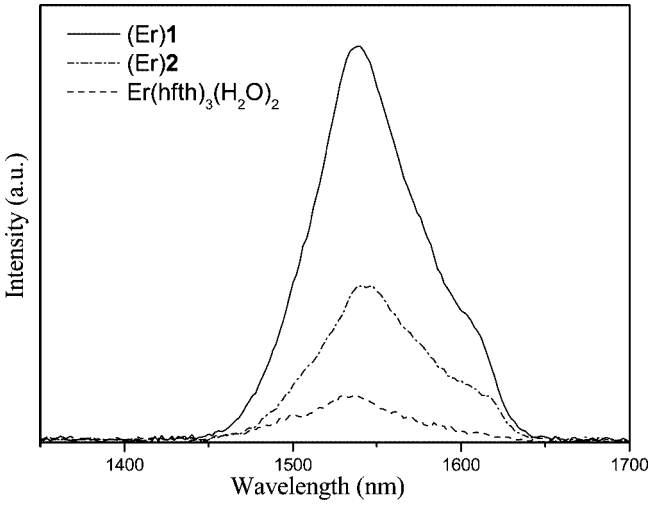

Figure 5. Emission spectra (λ_{ex} = 397 nm) of (Er)**1**, (Er)**2**, and $[Er(hfth)_3(H_2O)_2]$ (in the solid state as powder) at room temperature.

spectrum ranges extending from 1414 to 1664 nm and from 1448 to 1656 nm, respectively, with the emission maxima both located at 1540 nm. The emission obtained is attributed to the transition from the first excited state ($^4I_{13/2}$) to the ground state ($^4I_{15/2}$) of the partially filled 4f shell of the Er^{3+} ion (see the inset of Figure 4a). The erbium complexes are especially interesting for application in optical amplification because the transition around 1540 nm is in the right position for the third telecommunication window. To enable a wide-gain bandwidth for optical amplification, a broad emission band is desirable.[2d,21] The full widths at half maximum (FWHM) of the $^4I_{13/2} \rightarrow {}^4I_{15/2}$ transition for the (Er)**1** and (Er)**2** complexes are 76 and 74 nm, respectively, which enable a wide-gain bandwidth for optical amplification.[22]

Holmium

In the excitation spectra of (Ho)**1** and (Ho)**2** (Figure S2), the broad excitation bands in the UV region are both observed, which can be attributed to the absorption of the

 © 2006 Wiley-VCH Verlag GmbH & Co. KGaA, Weinheim

ligands. The excitation edge of the ligands overlaps some absorption bands corresponding to the characteristic transitions of the Ho^{3+} ion. These f–f transitions correspond to $^5I_8 \rightarrow {}^5G_4 + {}^3F_7$ (389 nm), $^5I_8 \rightarrow {}^5G_5$ (421 nm), $^5I_8 \rightarrow {}^5G_6 + {}^5F_1$ (453 nm), and $^5I_8 \rightarrow {}^5F_3$ (488 nm), which are in agreement with those of the DR spectra discussed above (Figure 4b).

Of importance is the observation of less frequently investigated NIR luminescence in holmium complexes.[1b,2e,23] The emission spectra of (Ho)**1** and (Ho)**2**, after ligand-mediated excitation at 397 nm, are shown in Figure 6. Both luminescence spectra consist of three bands at 990, 1200, and 1500 nm, which are attributed to the $^5F_5 \rightarrow {}^5I_7$, $^5I_6 \rightarrow {}^5I_8$, and $^5F_5 \rightarrow {}^5I_6$ transitions, respectively. For (Ho)**1** and (Ho)**2**, the intensity sequence of the bands is $I(^5F_5 \rightarrow {}^5I_7) > I(^5F_5 \rightarrow {}^5I_6) > I(^5I_6 \rightarrow {}^5I_8)$. As is shown in the energy diagram of the Ho^{3+} ion (inset of Figure 4b), the $^5I_7 \rightarrow {}^5I_8$ transition (>1900 nm) exceeds the measurement range of our detector. Since the optimum energy difference favors efficient ligand-to-ion energy transfer, it is supposed that the $^5F_4$, $^5S_2$, and $^5F_5$ levels are the main acceptor levels, and the excited electrons on the $^5F_5$ and $^5I_6$ levels could partially come from the relaxation of the upper levels followed by the transitions to the lower levels to give the NIR emission of the Ho^{3+} ion.[2e] Among these obtained NIR emissions, the 1500-nm emission is particularly attractive for its good agreement with the efficient working window of a quartz fiber. For the (Ho)**1** complex, the 1500-nm emission, which covers from 1420 to 1550 nm, may be due to the Stark splitting of the $^5F_5$ and $^5I_6$ levels, providing a satisfying waveband for the wavelength division multiplexing technology in optical communications.[2e] The FWHM of this emission is 62 nm, which is a broad bandwidth for the potential application of the optical communication systems.

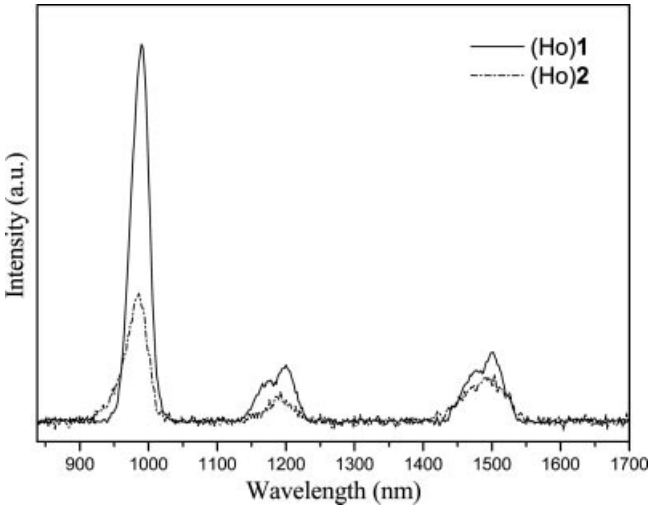

Figure 6. Emission spectra (λ_{ex} = 397 nm) of (Ho)**1** and (Ho)**2** (in the solid state as powder) at room temperature.

Ytterbium

The excitation spectra of (Yb)**1** and (Yb)**2** were obtained by monitoring the characteristic emission of the Yb^{3+} ion at 980 nm (Figure S2). The excitation spectra are dominated by a broad band ranging from 200 to 500 nm for both complexes. These two broad bands can be assigned to the absorption of the organic ligands and are in agreement with those in the DR spectra (Figure 4c). The emission spectra of the two complexes (Figure 7), after ligand-mediated excitation at 397 nm, clearly show the characteristic emission bands of the Yb^{3+} ion at 980 nm, which are assigned to the $^2F_{5/2} \rightarrow {}^2F_{7/2}$ transition. It should be noted that the Yb^{3+} ion emission in the two complexes is not a single sharp band but an envelope of bands arising at the lower energy side (1009 and 1038 nm) of the primary 980-nm emission band. A similar splitting has been reported previously.[24–26] According to the literature, these bands arise from the M_J splitting of the emitting and/or fundamental state as a consequence of ligand-field effects.[26]

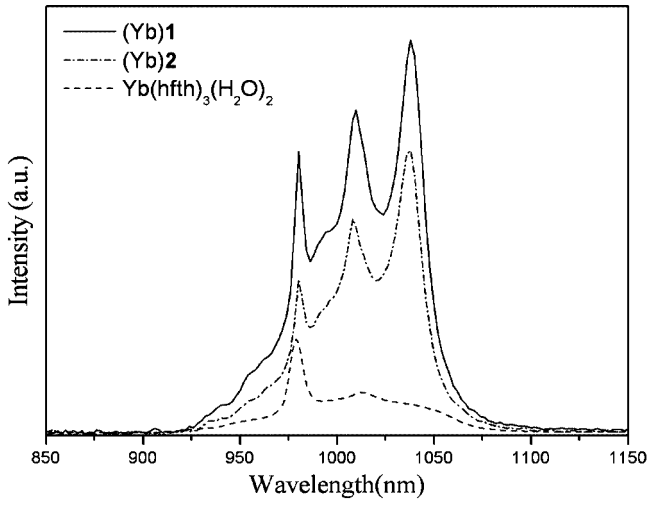

Figure 7. Emission spectra (λ_{ex} = 397 nm) of (Yb)**1**, (Yb)**2**, and $[Yb(hfth)_3(H_2O)_2]$ (in the solid state as powder) at room temperature.

The Yb^{3+} ion plays an important role in laser emission because of its very simple f–f energy level structure: besides the $^2F_{7/2}$ ground multiplet, there is only the $^2F_{5/2}$ excited multiplet at around 10000 cm^{-1}. There is no excited-state absorption on reducing the effective laser cross-section, no up-conversion, no concentration quenching, and no absorption in the visible range. The intense Yb^{3+} ion absorption lines are well suited for laser diode pumping in this range and the smaller Stokes shift (about 650 cm^{-1}) between absorption and emission reduces the thermal loading of the material during laser operation.[27] These properties of the Yb^{3+} ion and the obtained high intensity emission make these Yb complexes very important for various photonic applications in ionic crystals and glasses.[28] In addition, the relative transparency of human tissue at approximately 1000 nm suggests that in vivo luminescent probes operating at this wavelength (Yb-based emission) could have diagnostic value.[29]

Neodymium

In the excitation spectrum of (Nd)**2** (λ_{em} = 1061 nm), a broad band ranging from 260 to 498 nm due to the absorp-

 © 2006 Wiley-VCH Verlag GmbH & Co. KGaA, Weinheim

tion of the organic ligands superimposed with some excitation bands originating from the characteristic absorption transition of the Nd^{3+} ion is observed (Figure S2). These f–f transitions correspond to $^4I_{9/2}\rightarrow{}^2P_{1/2} + {}^2D_{5/2}$ (432 nm), $^4I_{9/2}\rightarrow{}^4G_{11/2} + {}^2K_{15/2} + {}^2G_{9/2} + {}^2D_{3/2}$ (474 nm), $^4I_{9/2}\rightarrow{}^4G_{9/2}$ (515 nm), and $^4I_{9/2}\rightarrow{}^2K_{13/2} + {}^4G_{7/2}$ (529 nm) of the Nd^{3+} ion, which are well in agreement with those of the DR spectrum (Figure 4d). It should be noted that these absorption transitions are much weaker than that of the ligands, which proves that luminescence sensitization by excitation of the ligands is much more efficient than direct excitation of the absorption levels of the Nd^{3+} ion.

The excitation of the Nd complex by strongly absorbing ligands (λ_{ex} = 397 nm) is quite feasible, as expected based on the energy level of the triplet state, which is higher than the Nd luminescent excited state $^4F_{3/2}$ (11527 cm^{-1}). The emission spectrum of the Nd complex (Figure 8) consists of three bands at λ = 880, 1061, and 1335 nm, which are attributed to the f–f transitions $^4F_{3/2}\rightarrow{}^4I_{9/2}$, $^4F_{3/2}\rightarrow{}^4I_{11/2}$, and $^4F_{3/2}\rightarrow{}^4I_{13/2}$, respectively. Some crystal-field fine structure can be observed, which is an indication that the Nd^{3+} ion occupies well-defined crystallographic sites in the complex.[23] Among the three emission bands of the Nd complex, the intensity of the transition at 1061 nm is the strongest and is potentially applicable for laser emission. The fine structure of the 1335-nm band of the complex offers the opportunity to develop new materials suitable for optical amplifiers operating at 1.3 μm.[30]

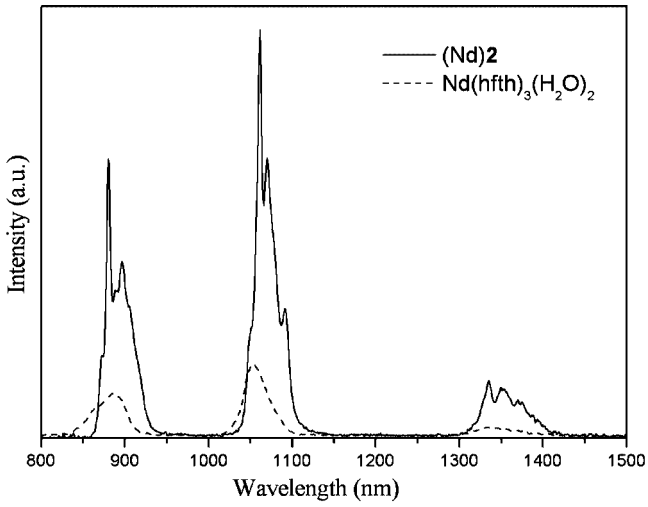

Figure 8. Emission spectra (λ_{ex} = 397 nm) of (Nd)**2** and [Nd(hfth)$_3$(H$_2$O)$_2$] (in solid state as powder) at room temperature.

Upon excitation of the ligand absorption band (397 nm), these lanthanide complexes all show the characteristic NIR luminescence of Ln^{3+} ions. The NIR luminescence obtained in this study shows that the ligands shield the lanthanide ions well from their surroundings and transfer energy from their triplet states to the Ln^{3+} ions efficiently.[31–34] Because no direct excitation of the lanthanide moiety occurs at the excitation wavelength (397 nm), the observed NIR emission signals only arise by sensitization of the lanthanide ions by the ligands.

Many authors have reported the influence of water on the intensity of Eu^{III} luminescence.[35] In fact, the NIR luminescence is even more sensitive to water than the visible luminescence. As shown in Figures 5, 7, and 8, respectively, an obvious decrease of the NIR-emission intensity for [Ln(hfth)$_3$(H$_2$O)$_2$] (Ln = Er, Yb, Nd) is detected when compared to the intensity of the corresponding (Ln)**1** or (Ln)**2** complex. This is probably related to the replacement of solvent molecules (ethanol or water) by phen or bipy in the Ln^{III} coordination sphere, which could depress nonradiative deactivation pathways through vibrational quenching.[36] These results suggest that the introduction of a second ligand instead of water molecules is able to increase the efficiency of energy transfer from the ligands to the central metal ions, thus resulting in an improvement in the emission intensity. In the meantime, it is worth noting that the relative emission intensity of (Ln)**1** is stronger than that of (Ln)**2** (Ln = Er, Ho, Yb). Basically, in the lanthanide complexes the ligands may sensitize the Ln^{3+} ion by energy transfer, and the probability of energy transfer is strongly influenced by the energy difference between the energy donor and acceptor.[37] The triplet-state energy level of bipy was measured and calculated to be 23095 cm^{-1} from the shortest-wavelength phosphorescence band of the phosphorescence spectrum for [Gd(bipy)$_3$Cl$_2$] (Figure S3, Supporting Information), in which the fine-structure is observed. We have measured the triplet energy states of the phen[38] and Hhfth[10c] ligands to be 22173 and 20400 cm^{-1}, respectively. So, the energy difference between the phen ligand and the Hhfth ligand is smaller than that between the bipy ligand and the Hhfth ligand. The phen ligand may transfer energy to hfth more efficiently and accordingly afford a stronger sensitization of the Ln^{3+} ion emission.[35a,39] In addition, all the C and N atoms of the phen molecule are located in the same conjugate area, yet those of the bipy molecule are not. It is therefore concluded that the presence of a rigid planar structure in the complex causes a higher intensity of the sensitized luminescence because such a structure allows a better energy transfer.[5] Therefore, the combination of phen and hfth ligands may sensitize the Ln^{3+} ion more efficiently, followed by the stronger NIR luminescence of the Ln^{3+} ion.

The luminescence decay curves obtained from time-resolved luminescence experiments could be fitted monoexponentially, thus confirming that the chemical environment of the Ln^{3+} ion is uniform in the materials.[20,40] The corresponding lifetimes of the lanthanide excited states are shown in Table 2. Due to the weakness of the signal and the limitations of our equipment, no reliable decay time could be measured for the Ho complexes. The quantum yields of the lanthanide-centered luminescence in these complexes were determined by taking [Yb(tta)$_3$phen] (tta = thenoyltrifluoroacetonate) as standard. The quantum yields (Q) of these complex samples (S) were calculated by using the following equation,[24c,41] where n is the refractive index

 © 2006 Wiley-VCH Verlag GmbH & Co. KGaA, Weinheim

of the solvent, I is the wavelength-integrated area of the corrected emission spectrum, and A is the absorbance value at the excitation wavelength.

$$Q_S = \frac{n_S^2 I_S A_R}{n_R^2 A_S I_R} Q_R$$

Table 2. Emission properties for the different NIR-emitting lanthanide complexes.

Complex	Transition	λ_{em} [nm]	τ [μs][a]	Q_S [%][b]
(Er)**1**	$^4I_{13/2}\rightarrow{}^4I_{15/2}$	1541	2.73	0.019
(Er)**2**	$^4I_{13/2}\rightarrow{}^4I_{15/2}$	1541	2.27	0.014
(Yb)**1**	$^2F_{5/2}\rightarrow{}^2F_{7/2}$	980	14.7	1.28
(Yb)**2**	$^2F_{5/2}\rightarrow{}^2F_{7/2}$	980	13.8	1.24
$Yb(hfth)_3(H_2O)_2$	$^2F_{5/2}\rightarrow{}^2F_{7/2}$	980	0.97	0.37
(Nd)**2**	$^4F_{3/2}\rightarrow{}^4I_{11/2}$	1061	1.27	0.072
$Nd(hfth)_3(H_2O)_2$	$^4F_{3/2}\rightarrow{}^4I_{11/2}$	1065	0.15	0.0085

[a] Luminescence lifetimes in the solid state. [b] Quantum yields of the solution of these complexes in toluene. The excitation wavelength is 355 nm.

The quantum yield of the reference (R), [Yb(tta)$_3$phen] in toluene solution (n = 1.4964), was taken as Q_R = 1.1%.[42] Then, the quantum yields of the solution of these complexes in toluene were obtained (Table 2). It can be seen that the quantum yields of these complexes in toluene increase in the order (Ln)**1** > (Ln)**2**, which agrees well with the corresponding lengthening of the emission lifetime. This correlation further shows that the combination of hfth and phen ligands may sensitize the Ln^{3+} ion more efficiently than the combination of hfth and bipy ligands. It should also be noted that the emission lifetimes and quantum yields for the Yb and Nd complexes investigated are considerably longer than those of the corresponding [Ln(hfth)$_3$(H$_2$O)$_2$] complexes, probably because the two water ligands (containing four potentially quenching O–H oscillators) have been replaced by phen or bipy, in which most of the C–H oscillators are remote from the metal center.

The luminescence lifetimes and quantum yield values obtained are in line with, or a little higher than, other recently published results on NIR-luminescent lanthanide complexes.[36,42,43] High-frequency oscillators, such as C–H vibrations in the ligand, can provide a very efficient nonradiative pathway for relaxation of the luminescent state of the NIR-emitting lanthanide ions by vibronic coupling, since it can be effectively mediated by the ubiquitous molecular vibrations. It would appear that the heptafluorinated substituent in the main sensitizer hfth serves to reduce the degree of vibrational quenching, which, in turn, probably leads to a slightly longer lived Ln^{3+} ion excited state. There still exists one C–H bond in the β-diketonate chelate ring of the complex, however, and this results in the main nonradiative factor. Suppression of such vibrational excitation in the system requires deuteration of the C–H bonds or replacement of C–H bonds with C–F bonds in the ligand.[7g] In addition, improvement of the spectral overlap of the NIR-emitting Ln^{3+} ion and the antenna and optimization of the luminescence quantum yield could be achieved by incorporating antenna chromophores with lower lying triplet states. This ligand feature is particularly important in the design of NIR-emitting lanthanide complexes.

Thermogravimetric Analyses

The TGA-DTA analyses of all the (Ln)**1** and (Ln)**2** complexes were carried out. The TGA diagrams of (Ln)**1** and (Ln)**2** are similar, and all reveal two main weight losses. (Yb)**1** and (Nd)**2** are given as examples in Figure 9. For (Yb)**1**, the analysis show that the melting point is 207.04 °C. The first weight loss of 74.02% is close to the calculated value (73.23%) corresponding to the loss of the hfth ligands and the second weight loss of 12.57% corresponds to the loss of the phen ligand (calculated: 13.65%). For (Nd)**2**, the analysis displays a first weight loss of 74.22% corresponding to the loss of hfth ligands (calculated: 76.23%) and a second weight loss of 12.23% corresponding to the loss of the bipy ligand (calculated: 12.33%). The final residues for (Yb)**1** and (Nd)**2** are composed of Yb_2O_3 and Nd_2O_3, respectively. The analyses show that the melting points of the (Ln)**1** and (Ln)**2** complexes are between 200 and 215 °C, and the decomposition temperatures are higher than 350 °C. These results suggest that these complexes have good thermal stability. This may be due to the heptafluorinated substituent in the ligand, as we and other authors have reported that a fluorinated substituent in a ligand leads to an improved thermal and oxidative stability and increases

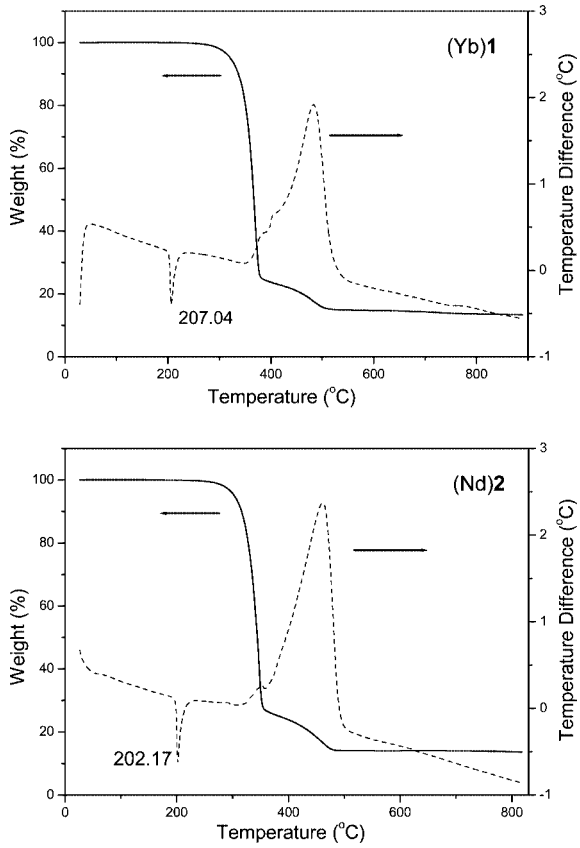

Figure 9. TGA (−) and DTA (---) curves of (Yb)**1** and (Nd)**2**.

 © 2006 Wiley-VCH Verlag GmbH & Co. KGaA, Weinheim

the volatility of the complex.[9,10c,44] The improved thermal stability and volatility result in good film-forming ability, which facilitates the fabrication of electroluminescent devices.

Conclusions

Based on the ligand hfth, seven new ternary lanthanide complexes (Ln)**1** (Ln = Er, Ho, Yb) and (Ln)**2** (Ln = Er, Ho, Yb, Nd) have been synthesized. Their single-crystal X-ray diffraction analyses [except (Er)**2**], growth morphology, DR spectra, optical properties, and TGA-DTA analyses have been reported. We have demonstrated the characteristic NIR luminescence of the corresponding lanthanide complexes upon excitation of the ligand absorption bands, mediated by the sensitizing effect of the ligands in the complexes, known as the antenna effect. The broadband emission at 1540 nm for the Er complexes, 1500 nm for the Ho complexes, and the fine structure at 1335 nm for the Nd complex offer the opportunities to develop new materials suitable for optical amplifiers operating at 1.5 and 1.3 μm, the two telecommunications windows. The heptafluorinated substituent in the main sensitizer hfth serves to reduce the degree of vibrational quenching. In addition, improvement of the spectral overlap of the NIR-emitting Ln^{3+} ion and the antenna and optimization of the luminescence quantum yield could be achieved by incorporating antenna chromophores with lower lying triplet states. This ligand feature is particularly important in the design of NIR-emitting lanthanide complexes and further work is in process. Furthermore, the above results are pertinent to the application of these complexes in NIR electroluminescent devices. In ongoing work, we are exploring the properties of electroluminescent devices fabricated using these lanthanide complexes as the active materials.

Experimental Section

Materials: Ytterbium oxide (Yb_2O_3, 99.99%), neodymium oxide (Nd_2O_3, 99.99%), holmium oxide (Ho_2O_3, 99.99%), erbium oxide (Er_2O_3, 99.99%), and gadolinium oxide (Gd_2O_3, 99.99%) were purchased from Yue Long Chemical Plant (Shanghai, China). Sodium metal (≥98%, A. R.), 1,10-phenanthroline monohydrate (phen·H_2O, 99%, A. R.), and 2,2′-bipyridine (≥99.5%, A. R.) were bought from Beijing Fine Chemical Co. (Beijing, China). Hhfth was purchased from Acros Organics Co. (Geel, Belgium) and Htta (2-thenoyltrifluoroacetone) from Aldrich. All these reagents were used directly without further purification. The toluene solvent was dried by a standard procedure (with Na/benzophenone), distilled under nitrogen, and kept over molecular sieves. The $LnCl_3$ (Ln = Er, Ho, Yb, Nd, Gd) ethanol solution was prepared as follows: the rare earth oxide (Ln_2O_3) was dissolved in concentrated hydrochloric acid (HCl) and the surplus HCl was removed by evaporation. The residue was diluted with anhydrous ethanol. The concentration of the rare earth ion was measured by titration with a standard EDTA (ethylenediaminetetraacetic acid) aqueous solution.

Instrumentation: The CHN elemental analyses were carried out with a VarioEL analyzer. The DR measurements were performed with a Hitachi U-4100 spectrophotometer. The UV/Vis absorption spectra (solutions of Hhfth and bipy in ethanol; solutions of the investigated complexes in toluene) were recorded with a TU-1901 spectrophotometer. The excitation and emission spectra were measured with an Edinburgh Analytical Instruments FLS920 equipped with a laser diode (LD) from the PicoQuant Company as the light source. The time-resolved measurements for the Yb and Nd complexes were performed with an Edinburgh Analytical Instruments FLS920 equipped with a 397-nm picosecond laser diode (LD) from the PicoQuant Company and for Er complexes with an Edinburgh Combined Fluorescence Lifetime and Steady State Spectrometer FLS920 equipped with a μF900 lamp (λ_{ex} = 397 nm). Freshly collected (Er)**1** crystals were mounted on the glass and were observed and recorded with an infrared microscope (HYPERION 3000) from German Bruker Company. All measurements were performed at room temp. The low-temperature phosphorescence spectrum of the Gd^{3+} complex was measured with a Hitachi F-4500 spectrophotometer at liquid nitrogen temperature (77 K). The TGA-DTA analyses were measured with an SDT 2960 Simultaneous DSC-TGA of American TA Instruments, with a heating rate of 10 °C min^{-1}.

Synthesis of the (Ln)1 Complexes (Ln = Er, Ho, Yb): Hhfth (190 μL, 0.9 mmol) and phen·H_2O (0.0595 g, 0.3 mmol) were dissolved in a suitable volume of anhydrous ethanol. Then, an appropriate amount of 1.0 M sodium hydroxide solution was added dropwise to the solution to adjust the pH value to approximately 7. $LnCl_3$ ethanol solution (0.3 mmol), prepared separately, was then added dropwise to this mixture with stirring. The mixture was heated to reflux and kept at 78 °C for 6 h, and then cooled to the room temperature. The precipitates were collected by filtration, washed with water and ethanol, and dried at 70 °C under vacuum overnight. The lanthanide complex was recrystallized from an ethanol/acetone mixture. Pink (for erbium), pale-yellow (for ytterbium), or yellow crystals (for holmium) suitable for X-ray single-crystal structural determination were grown from the mother liquor at room temp.

Synthesis of the (Ln)2 Complexes (Ln = Er, Ho, Yb, Nd): The procedure used to prepare the (Ln)**2** was the same as that used for the (Ln)**1** complex expect that bipy (0.0469 g, 0.3 mmol) was dissolved in anhydrous ethanol instead of phen·H_2O (0.0595 g, 0.3 mmol). The (Ln)**2** complex obtained was also recrystallized from an ethanol/acetone mixture. Lilac (for neodymium), pale-yellow (for ytterbium), or yellow crystals (for holmium) suitable for X-ray single-crystal structural determination were grown from the mother liquor at room temp. The purity of the compounds was verified by CHN elemental analysis (Table S1, Supporting Information).

Synthesis of the [Ln(hfth)$_3$(H$_2$O)$_2$] Complexes (Ln = Er, Ho, Yb, Nd): An appropriate amount of 1.0 M sodium hydroxide solution was added dropwise to an Hhfth (190 μL, 0.9 mmol) ethanol solution whilst stirring to adjust the pH value to approximately 7. The $LnCl_3$ ethanol solution (0.3 mmol) was added dropwise to this mixture with stirring. Then, an appropriate amount of water was added and the mixture was heated to reflux and kept at 60 °C for 6 h. The rest of the procedure was similar to that used for the (Ln)**1** complex. All complexes were found to be dihydrates.

Synthesis of [Gd(bipy)$_3$Cl$_2$]: At room temperature, 1.5 mmol of bipy was dissolved in a suitable volume of anhydrous ethanol. Then, 0.5 mmol of a $GdCl_3$ ethanol solution was added whilst stirring and the solution was heated under reflux for 2 h. The white powder was filtered and washed with ethanol. The resulting complex was dried at 60 °C under vacuum overnight.

Synthesis of [Yb(tta)$_3$phen]: This complex was synthesized according to a published method.[45]

 © 2006 Wiley-VCH Verlag GmbH & Co. KGaA, Weinheim

Table 3. Crystal data and structure refinement for (Ln)**1** and (Ln)**2** [except (Er)**2**].

	(Ho)**1**	(Er)**1**	(Yb)**1**	(Nd)**2**	(Ho)**2**	(Yb)**2**
Empirical formula	$C_{42}H_{20}F_{21}HoN_2O_6S_3$	$C_{42}H_{20}ErF_{21}N_2O_6S_3$	$C_{42}H_{20}F_{21}N_2O_6S_3Yb$	$C_{40}H_{20}F_{21}N_2NdO_6S_3$	$C_{40}H_{20}F_{21}HoN_2O_6S_3$	$C_{40}H_{20}F_{21}N_2O_6S_3Yb$
Formula mass	1308.71	1311.04	1316.82	1264.00	1284.69	1292.80
T [K]	293(2)	187(2)	187(2)	187(2)	187(2)	187(2)
λ [Å]	0.71073	0.71073	0.71073	0.71073	0.71073	0.71073
Crystal system	orthorhombic	orthorhombic	orthorhombic	orthorhombic	orthorhombic	orthorhombic
Space group	*Pbca*	*Pbca*	*Pbca*	*Pbca*	*Pbca*	*Pbca*
a [Å]	20.9790(5)	20.6146(9)	20.6224(9)	19.9666(12)	19.8709(7)	19.8161(9)
b [Å]	18.3620(5)	18.0507(8)	18.0173(8)	18.4175(11)	18.1779(6)	18.0740(8)
c [Å]	25.5920(5)	25.5197(12)	25.5224(11)	25.3703(15)	25.5521(9)	25.6376(11)
α [°]	90	90	90	90	90	90
β [°]	90	90	90	90	90	90
γ [°]	90	90	90	90	90	90
V [Å^3]	9858.4(6)	9496.1(7)	9483.1(7)	9329.5(10)	9229.7(6)	9182.3(7)
Z	8	8	8	8	8	8
$D_{calcd.}$ [mg m^{-3}]	1.763	1.834	1.845	1.800	1.849	1.870
Abs. coeff. [mm^{-1}]	1.859	2.031	2.236	1.379	1.984	2.307
F(000)	5104	5112	5128	4952	5008	5032
Crystal size [mm]	0.53×0.34×0.19	0.33×0.27×0.17	0.35×0.29×0.14	0.33×0.12×0.05	0.25×0.27×0.15	0.26×0.16×0.10
θ range [°]	1.59 to 28.29	1.70 to 26.03	1.70 to 26.04	1.61 to 25.08	1.59 to 26.05	1.59 to 28.65
Reflns collected	59772	51450	51480	46137	50058	55491
Ind. reflns (R_{int})	11819 (0.0447)	9368 (0.0601)	9342 (0.0213)	8274 (0.1044)	9118 (0.0445)	11192 (0.0876)
Refinement method	full-matrix least squares on F^2					
Data/restraints/parameters	11819/26/631	9368/4/685	9342/56/638	8274/37/505	9118/24/667	11192/23/667
GOF on F^2	1.038	1.061	1.012	1.037	1.023	0.931
R_1 [$I > 2\sigma(I)$]	0.0713	0.0554	0.0679	0.1240	0.0553	0.0568
wR_2 [$I > 2\sigma(I)$]	0.2404	0.1631	0.1952	0.3134	0.1611	0.1428
R_1 (all data)	0.1217	0.0727	0.0777	0.1831	0.0783	0.1043
wR_2 (all data)	0.2734	0.1754	0.2050	0.3579	0.1769	0.1643

Single-Crystal X-ray Diffraction Study: X-ray data for the selected crystal mounted on a glass fiber were collected with a CCD area detector with graphite-monochromated Mo-K_α radiation. Reflections were collected with a Bruker SMART APEX detector and processed with SAINT from Bruker. Data were corrected for Lorentz and polarization effects. The structure was solved by direct methods and expanded using Fourier techniques. The non-hydrogen atoms [for (Yb)**1** except F3–F7, F17–F21; for (Nd)**2** except F atoms] were refined anisotropically. The hydrogen atoms were included using a riding model. All calculations were performed using the SHELXL-97 crystallographic software package.[46] For the crystallographic data some R values are high, and for the ORTEP plots some of the ellipsoids of some fluorine atoms have a very irregular shape. These problems could be due to the poor X-ray data and disorder of the fluorine atoms. Crystallographic data and structural refinements for compounds (Ln)**1** and (Ln)**2** are summarized in Table 3. CCDC-266576 [for (Ho)**2**], -266577 [for (Ho)**1**], -266578 [for (Er)**1**], -266579 [for (Yb)**2**], -266816 [for (Yb)**1**], and -266983 [for (Nd)**2**] contain the supplementary crystallographic data for this paper. These data can be obtained free of charge from The Cambridge Crystallographic Data Centre via www.ccdc.cam.ac.uk/data_request/cif.

Supporting Information (see footnote on the first page of this article): Molecular structures of the complexes (Ln)**1** and (Ln)**2** (Figure S1), excitation spectra of (Ln)**1** and (Ln)**2** complexes (Ln = Er, Ho, Yb, Nd) and absorption spectra of the ligands (phen, Hhfth and bipy) (Figure S2), phosphorescence spectrum of $[Gd(bipy)_3Cl_2]$ (Figure S3), results of elemental analyses of complexes (Ln)**1** and (Ln)**2** (Table S1).

Acknowledgments

This work was supported by the National Natural Science Foundation of China (grant nos. 20372060, 20131010, 20490210, 20340420326) and financial aid from MOST of China ("973" Program, no. 2006CB601103). We are grateful to Dr. E. Ma and Prof. J. G. Mao of the Fujian Institute of Research on the Structure of Matter, Chinese Academy of Sciences, and Prof. Q. Su and Dr. L. Feng of Sun Yat-sen University for assistance with the fluorescence measurements. We also thank Dr. D. M. Wang and Dr. Y. J. Zhang (Changchun Institute of Applied Chemistry) for their help with the microscope pictures of the crystals.

[1] a) S. Kim, Y. T. Lim, E. G. Soltesz, A. M. De Grand, J. Lee, A. Nakayama, J. A. Parker, T. Mihaljevic, R. G. Laurence, D. M. Dor, L. H. Cohn, M. G. Bawendi, J. V. Frangioni, *Nat. Biotechnol.* **2004**, *22*, 93–97; b) J. Zhang, P. D. Badger, S. J. Geib, S. Petoud, *Angew. Chem. Int. Ed.* **2005**, *44*, 2508–2512.

[2] a) L. N. Sun, H. J. Zhang, Q. G. Meng, F. Y. Liu, L. S. Fu, C. Y. Peng, J. B. Yu, G. L. Zheng, S. B. Wang, *J. Phys. Chem. B* **2005**, *109*, 6174–6182; b) T. J. Foley, B. S. Harrison, A. S. Knefely, K. A. Abboud, J. R. Reynolds, K. S. Schanze, J. M. Boncella, *Inorg. Chem.* **2003**, *42*, 5023–5032; c) W. D. Horrocks Jr, J. P. Bolender, W. D. Smith, R. M. Supkowski, *J. Am. Chem. Soc.* **1997**, *119*, 5972–5973; d) M. P. O. Wolbers, F. C. J. M. van Veggel, B. H. M. Snellink-Ruël, J. W. Hofstraat, F. A. J. Geurts, D. N. Reinhoudt, *J. Chem. Soc., Perkin Trans. 2* **1998**, 2141–2150; e) F. X. Zang, W. L. Li, Z. R. Hong, H. Z. Wei, M. T. Li, X. Y. Sun, C. S. Lee, *Appl. Phys. Lett.* **2004**, *84*, 5115–5117; f) G. A. Casay, D. B. Shealy, G. Patonay, *Near-*

 © 2006 Wiley-VCH Verlag GmbH & Co. KGaA, Weinheim

Infrared Fluorescence Probes, Plenum Press, New York, London, **1994**, vol, 4, p. 183–222; g) L. H. Slooff, A. Polman, M. P. Oude Wolbers, F. C. J. M. van Veggel, D. N. Reinhoudt, J. W. Hofstraat, *J. Appl. Phys.* **1997**, *83*, 497–503; h) M. H. V. Werts, J. W. Hofstraat, F. A. J. Geurts, J. W. Verhoeven, *Chem. Phys. Lett.* **1997**, *276*, 196–201.

[3] a) M. Kawa, J. M. J. Fréchet, *Chem. Mater.* **1998**, *10*, 286–296; b) C. Piguet, J.-C. G. Bünzli, G. Bernardinelli, G. Hopfgartner, A. F. Williams, *J. Am. Chem. Soc.* **1993**, *115*, 8197–8206.

[4] a) S. I. Weissman, *J. Chem. Phys.* **1942**, *10*, 214–217; b) G. A. Crosby, R. E. Whan, J. J. Freeman, *J. Phys. Chem.* **1962**, *66*, 2493–2499.

[5] K. Binnemans, in *Handbook on the Physics and Chemistry of Rare Earths* (Eds.: K. A. Gschneidner Jr, J.-C. G. Bünzli, V. K. Pecharsky), Elsevier, Amsterdam, **2005**, vol. 35, chapter 225, p. 107–272.

[6] I. K. Hemmilä, *Applications of Fluorescence in Immunoassays*, Wiley and Sons, New York, **1991**.

[7] a) G. Mancino, A. J. Ferguson, A. Beeby, N. J. Long, T. S. Jones, *J. Am. Chem. Soc.* **2005**, *127*, 524–525; b) G. E. Buono-Core, H. Li, B. Marciniak, *Coord. Chem. Rev.* **1990**, *99*, 55–87; c) J. H. Melman, T. J. Emge, J. G. Brennan, *Inorg. Chem.* **2001**, *40*, 1078–1081; d) Y. Hasegawa, T. Ohkubo, K. Sogabe, Y. Kawamura, Y. Wada, N. Nakashima, S. Yanagida, *Angew. Chem. Int. Ed.* **2000**, *39*, 357–360; e) J.-C. G. Bünzli, C. Piguet, *Chem. Soc. Rev.* **2005**, *34*, 1048–1077; f) A.-S. Chauvin, F. Gumy, I. Matsubayashi, Y. Hasegawa, J.-C. G. Bünzli, *Eur. J. Inorg. Chem.* **2006**, 473–480; g) S. Yanagida, Y. Hasegawa, K. Murakoshi, Y. Wada, N. Nakashima, T. Yamanaka, *Coord. Chem. Rev.* **1998**, *171*, 461–480.

[8] a) Y. X. Zheng, J. Lin, Y. J. Liang, Q. Lin, Y. N. Yu, Q. G. Meng, Y. H. Zhou, S. B. Wang, H. Y. Wang, H. J. Zhang, *J. Mater. Chem.* **2001**, *11*, 2615–2619; b) Y. Hasegawa, Y. Kimura, K. Murakoshi, Y. Wada, J. H. Kim, N. Nakashima, T. Yamanaka, S. Yanagida, *J. Phys. Chem.* **1996**, *100*, 10201–10205; c) J. L. Yuan, K. Matsumoto, *Anal. Sci.* **1996**, *12*, 31–36.

[9] J. B. Yu, L. Zhou, H. J. Zhang, Y. X. Zheng, H. R. Li, R. P. Deng, Z. P. Peng, Z. F. Li, *Inorg. Chem.* **2005**, *44*, 1611–1618.

[10] a) L. N. Sun, H. J. Zhang, L. S. Fu, F. Y. Liu, Q. G. Meng, C. Y. Peng, J. B. Yu, *Adv. Funct. Mater.* **2005**, *15*, 1041–1048; b) Y. X. Zheng, Y. H. Zhou, J. B. Yu, Y. N. Yu, H. J. Zhang, W. P. Gillin, *J. Phys. D: Appl. Phys.* **2004**, *37*, 531–534; c) Y. X. Zheng, L. S. Fu, Y. H. Zhou, J. B. Yu, Y. N. Yu, S. B. Wang, H. J. Zhang, *J. Mater. Chem.* **2002**, *12*, 919–923; d) L. N. Sun, H. J. Zhang, L. S. Fu, F. Y. Liu, Q. G. Meng, C. Y. Peng, J. B. Yu, S. B. Wang, *J. Rare Earths* **2004**, *22*, 812–815.

[11] a) R. Van Deun, D. Moors, B. De Fré, K. Binnemans, *J. Mater. Chem.* **2003**, *13*, 1520–1522; b) R. Van Deun, P. Fias, P. Nockemann, A. Schepers, T. N. Parac-Vogt, K. Van Hecke, L. Van Meervelt, K. Binnemans, *Inorg. Chem.* **2004**, *43*, 8461–8469.

[12] a) C. Tedeschi, J. Azéma, H. Gornitzka, P. Tisnès, C. Picard, *Dalton Trans.* **2003**, 1738–1745; b) J. A. Fernandes, R. A. Sá Ferreira, M. Pillinger, L. D. Carlos, I. S. Gonçalves, P. J. A. Ribeiro-Claro, *Eur. J. Inorg. Chem.* **2004**, 3913–3919.

[13] J. B. Yu, H. J. Zhang, L. S. Fu, R. P. Deng, L. Zhou, H. R. Li, F. Y. Liu, H. L. Fu, *Inorg. Chem. Commun.* **2003**, *6*, 852–854.

[14] J.-C. G. Bünzli, P. Froidevaux, C. Piguet, *New J. Chem.* **1995**, *19*, 661–668.

[15] a) M. Benatsou, B. Capoen, M. Bouazaoui, W. Tchana, J. P. Vilcot, *Appl. Phys. Lett.* **1997**, *71*, 428–430; b) V. V. Filippov, P. P. Pershukevich, V. V. Kuznetsova, V. S. Homenko, *J. Lumin.* **2002**, *99*, 185–195; c) J. A. Capobianco, F. Vetrone, J. C. Boyer, A. Speghini, M. Bettinelli, *J. Phys. Chem. B* **2002**, *106*, 1181–1187.

[16] a) K. Binnemans, H. De Leebeeck, C. Görller-Walrand, J. L. Adam, *Chem. Phys. Lett.* **1999**, *303*, 76–80; b) F. S. Liu, Q. L. Liu, J. K. Liang, J. Luo, L. T. Yang, G. B. Song, Y. Zhang, L. X. Wang, J. N. Yao, G. H. Rao, *J. Lumin.* **2005**, *111*, 61–68; c) M. Malinowski, Z. Frukacz, M. Szuflińska, A. Wnuk, M. Kaczkan, *J. Alloys Compd.* **2000**, *300–301*, 389–394.

[17] a) W. T. Carnall, P. R. Fields, K. Rajnak, *J. Chem. Phys.* **1968**, *49*, 4424–4442; b) G. F. Wang, W. Z. Chen, Z. B. Li, Z. S. Hu, *Phys. Rev. B* **1999**, *60*, 15469–15471; c) H. D. Jiang, J. Y. Wang, H. J. Zhang, X. B. Hu, H. Liu, *J. Appl. Phys.* **2002**, *92*, 3647–3650; d) V. Mehta, G. Aka, A. L. Dawar, A. Mansingh, *Opt. Mater.* **1999**, *12*, 53–63.

[18] a) K. Driesen, P. Nockemann, K. Binnemans, *Chem. Phys. Lett.* **2004**, *395*, 306–310; b) C. L. Maupin, R. S. Dickins, L. G. Govenlock, C. E. Mathieu, D. Parker, J. A. G. Williams, J. P. Riehl, *J. Phys. Chem. A* **2000**, *104*, 6709–6717.

[19] a) V. Bekiari, P. Lianos, *Adv. Mater.* **1998**, *10*, 1455–1458; b) N. Sabbatini, A. Mecati, M. Guardigli, V. Balzani, J. M. Lehn, R. Zeissel, R. Ungaro, *J. Lumin.* **1991**, *48–49*, 463–468; c) N. Sabbatini, M. Guardigli, J. M. Lehn, *Coord. Chem. Rev.* **1993**, *123*, 201; d) K. Driesen, R. Van Deun, C. Görller-Walrand, K. Binnemans, *Chem. Mater.* **2004**, *16*, 1531–1535.

[20] H. R. Li, J. Lin, H. J. Zhang, L. S. Fu, Q. G. Meng, S. B. Wang, *Chem. Mater.* **2002**, *14*, 3651–3655.

[21] R. Van Deun, P. Nockemann, C. Görller-Walrand, K. Binnemans, *Chem. Phys. Lett.* **2004**, *397*, 447–450.

[22] a) O. H. Park, S. Y. Seo, J. I. Jung, J. Y. Bae, B. S. Bae, *J. Mater. Res.* **2003**, *18*, 1039–1042; b) O. H. Park, S. Y. Seo, B. S. Bae, J. H. Shin, *Appl. Phys. Lett.* **2003**, *82*, 2787–2789.

[23] J. W. Stouwdam, F. C. J. M. van Veggel, *Nano Lett.* **2002**, *2*, 733–737.

[24] a) P. Lenaerts, K. Driesen, R. Van Deun, K. Binnemans, *Chem. Mater.* **2005**, *17*, 2148–2154; b) M. P. Tsvirko, G. F. Stelmakh, V. E. Pyatosin, K. N. Solovyov, T. F. Kachura, *Chem. Phys. Lett.* **1980**, *73*, 80–83; c) S. Quici, M. Cavazzini, G. Marzanni, G. Accorsi, N. Armaroli, B. Ventura, F. Barigelletti, *Inorg. Chem.* **2005**, *44*, 529–537.

[25] W. G. Perkins, G. A. Crosby, *J. Chem. Phys.* **1965**, *42*, 407–414.

[26] F. R. G. e Silva, O. L. Malta, C. Reinhard, H.-U. Güdel, C. Piguet, J. E. Moser, J.-C. G. Bünzli, *J. Chem. Phys. A* **2002**, *106*, 1670–1677.

[27] G. Boulon, A. Collombet, A. Brenier, M. T. Cohen-Adad, A. Yoshikawa, K. Lebbou, J. H. Lee, T. Fukuda, *Adv. Funct. Mater.* **2001**, *11*, 263–270.

[28] C. Reinhard, H. U. Güdel, *Inorg. Chem.* **2002**, *41*, 1048–1055.

[29] G. M. Davies, R. J. Aarons, G. R. Motson, J. C. Jeffery, H. Adams, S. Faulkner, M. D. Ward, *Dalton Trans.* **2004**, 1136–1144.

[30] a) S. I. Klink, P. O. Alink, L. Grave, F. G. A. Peters, J. W. Hofstraat, F. Geurts, F. C. J. M. van Veggel, *J. Chem. Soc., Perkin Trans. 2* **2001**, 363–372; b) W. P.-W. Lai, W.-T. Wong, *New J. Chem.* **2000**, *24*, 943–944.

[31] A. Beeby, S. Faulkner, D. Parker, J. A. G. Williams, *J. Chem. Soc., Perkin Trans. 2* **2001**, 1268–1273.

[32] N. Sabbatini, M. T. Indelli, M. T. Gandolfi, V. Balzani, *J. Phys. Chem.* **1982**, *86*, 3585–3591.

[33] O. L. Malta, F. R. G. e Silva, *Spectrochim. Acta Part A* **1998**, *54*, 1593–1599.

[34] F. R. G. e Silva, O. L. Malta, *J. Alloys Compd.* **1997**, *250*, 427–430.

[35] a) S. T. Frey, M. L. Gong, W. D. Horrocks Jr, *Inorg. Chem.* **1994**, *33*, 3229–3234; b) Y. X. Zheng, J. Lin, Y. J. Liang, Y. N. Yu, Y. H. Zhou, C. Guo, S. B. Wang, H. J. Zhang, *J. Alloys Compd.* **2002**, *336*, 114–118; c) Y. Haas, G. Stein, *J. Phys. Chem.* **1971**, *75*, 3677–3681; d) P. C. R. Soares-Santos, H. I. S. Nogueira, V. Félix, M. G. B. Drew, R. A. Sá Ferreira, L. D. Carlos, T. Trindade, *Chem. Mater.* **2003**, *15*, 100–108.

[36] N. M. Shavaleev, G. Accorsi, D. Virgili, Z. R. Bell, T. Lazarides, G. Calogero, N. Armaroli, M. D. Ward, *Inorg. Chem.* **2005**, *44*, 61–72.

[37] G. A. Crosby, R. E. Whan, R. M. Alire, *J. Chem. Phys.* **1961**, *34*, 743–748.

[38] C. Y. Peng, H. J. Zhang, J. B. Yu, Q. G. Meng, L. S. Fu, H. R. Li, L. N. Sun, X. M. Guo, *J. Phys. Chem. B* **2005**, *109*, 15278–15287.

 © 2006 Wiley-VCH Verlag GmbH & Co. KGaA, Weinheim

[39] Y. T. Yang, Q. D. Su, G. W. Zhao, *Spectrochim. Acta Part A* **1999**, *55*, 1527–1533.
[40] H. R. Li, J. Lin, H. J. Zhang, H. C. Li, L. S. Fu, Q. G. Meng, *Chem. Commun.* **2001**, 1212–1213.
[41] M. H. V. Werts, R. T. F. Jukes, J. W. Verhoeven, *Phys. Chem. Chem. Phys.* **2002**, *4*, 1542–1548.
[42] L. N. Puntus, K. J. Schenk, J.-C. G. Bünzli, *Eur. J. Inorg. Chem.* **2005**, 4739–4744.
[43] a) N. M. Shavaleev, S. J. A. Pope, Z. R. Bell, S. Faulkner, M. D. Ward, *Dalton Trans.* **2003**, 808–814; b) M. H. V. Werts, J. W. Verhoeven, J. W. Hofstraat, *J. Chem. Soc., Perkin Trans. 2* **2000**, 433–439.
[44] a) V. V. Grushin, N. Herron, D. D. LeCloux, W. J. Marshall, V. A. Petrov, Y. Wang, *Chem. Commun.* **2001**, 1494–1495; b) M. A. Omary, M. A. Rawashdeh-Omary, H. V. K. Diyabalanage, H. V. R. Dias, *Inorg. Chem.* **2003**, *42*, 8612–8614; c) I. R. Lasker, T.-M. Chen, *Chem. Mater.* **2004**, *16*, 111–117; d) H. V. R. Dias, W. Jin, *Inorg. Chem.* **1996**, *35*, 3687–3694; e) M. Becht, T. Gerfin, K. H. Dahmen, *Chem. Mater.* **1993**, *5*, 137–144.
[45] L. R. Melby, N. J. Rose, E. Abramson, J. C. Caris, *J. Am. Chem. Soc.* **1964**, *86*, 5117–5125.
[46] M. D. Regulacio, N. Tomson, S. L. Stoll, *Chem. Mater.* **2005**, *17*, 3114–3121.

Received: April 13, 2006
Published Online: August 7, 2006

 © 2006 Wiley-VCH Verlag GmbH & Co. KGaA, Weinheim